Journal of the European Ceramic Society 21 (2001) 841–845

www.elsevier.com/locate/jeurceramsoc

Creep behavior of SiC whisker-reinforced Si_3N_4/BN fibrous monolithic ceramics

Shuqin Li *, Yong Huang, Changan Wang, Yongming Luo, Linhua Zou, Cuiwei Li

State Key Lab of New Ceramics and Fine Processing, Department of Materials Science and Engineering, Tsinghua University, Beijing 100084, People's Republic of China

Received 15 June 2000; received in revised form 11 August 2000; accepted 21 August 2000

Abstract

The flexural creep behavior of SiC-whisker reinforced hot-pressed Si_3N_4/BN fibrous monolithic ceramics in the temperature range 1000–1200°C and stress range 250–600 MPa were characterized. Creep curves generally showed extensive primary and lack of tertiary creep. The creep and fracture mechanism were mainly controlled by the BN interlayer. BN began to oxidise at 1200°C and decreased the creep resistance. Meanwhile SiC whisker pulling-out improved the creep resistance. Microscopic damage mechanisms were investigated by SEM.

Keywords: BN; Composites; Creep; SiC whiskers; Si_3N_4/BN fibrous monoliths

1. Introduction

Silicon nitride-based ceramics possess excellent properties,[1,2] which make them ideal candidate materials for high temperature applications. However, the nature of brittleness is one of the most crucial problems in their applications.

Enlightened from studying some natural composites, e.g. bamboo, mollusk shell etc., ceramic matrix composites containing weak interfacial layers have been considered to offer a very important approach to improve the property of ceramics.[3,4] Whisker reinforcement is a well established method of enhancing the creep resistance of ceramic materials.[5,6] For this reason, the present investigation was designed to characterize the creep and creep fracture properities of Si_3N_4/BN fibrous monolithic ceramics. The creep responses at various temperatures and stress levels were measured. From the data, the kinetics of deformation and the stress dependence of flexural creep were determined. A numerical analysis was also employed to estimate the power-law creep parameters. The influence of microstructure on the creep deformation mechanisms was also investigated.

2. Experimental methods

2.1. Raw materials and fabrication process

Si_3N_4 (Founder High-Tech ceramic Corp., China) powders with 8 wt.% Y_2O_3 (purity >99.9%), 4 wt.% Al_2O_3 (>99.9%) were ball milled with 20 wt.% SiC whisker (TWS-400, Tokai Carbon Co., Japan) in ethanol for 24 h to achieve a homogenous mixture. This was mixed with organic binders and then produced green filaments using a coextrusion process. The green filaments were subsequently coated with a slurry of 25 wt.% BN and 75 wt.% Al_2O_3, dried and parallel packed into a graphite die. After dewaxing, the green body was hot pressed in a graphite resistance furnace under N_2 at 1820°C for 1.5 h and under a pressure of 22 MPa. A detailed description of the fabrication process can be found in the literature.[7] The test specimens were cut into 4×3×36 mm rectangular bars, then polished with diamond pastes down to 7 μm.

2.2. Creep testing

Creep testing was conducted using a creep tester which consisted of a three-point bend test fixture of α-SiC with a span of 30 mm. Loads were applied to the upper ram via a lever arm having a 5:1 leverage ratio.

* Corresponding author.
E-mail address: shuqinl@263.net (S. Li).

0955-2219/01/$ - see front matter
PII: S0955-2219(00)00251-X

Load-point deflections to center-point deflections of creeping specimens were measured directly using linear variable displacement transducer (LVDT). In the experiment, the rate of rising temperature was 500°C/h, and before the load was applied, the time of constant temperature was 15 min. Samples were creep tested between 1000 and 1200°C at stresses between 250 and 600 MPa under an air atmosphere. After testing, the tensile zones of the specimens were examined using X-ray diffraction (XRD) to determine the phases in the materials and by scanning electron microscopy to characterize the creep deformation mechanisms.

3. Results and discussion

3.1. Creep response

In this study, creep behavior of Si_3N_4/BN fibrous monolithic ceramics was systematically investigated in the temperature range 1000–1200°C. Test conditions and rupture times are shown in Table 1 and typical creep curves at 1200°C are shown in Fig. 1.

An obvious feature exhibited by these creep curves is their extensive primary creep and the lack of tertiary creep. There was a substantial primary creep response, which, in fact, accounts for most of the measured strain. The large primary creep response related to stress redistribution processes occurring in the composite and to the intrinsic response of glass-ceramic.[8,9] This redistrution of stress may involve one or more of the following processes: redistribution of residual intergranular glass phase and/or compliance of interface. Mayer et al.[9] systematically explored the role of the interface response in the composites. From their experiment, they concluded that plastic flow of an interface layer of siliconous glass emulated a debonded interface and contributed substantially to the observed creep response, although most of the primary strain reportedly derived from redistribution of the intergranular matrix glass. In the present study, the weak interfacial bond provided by the BN interlayer facilitated the redistribution of stress in a similar fashion during primary creep, particularly in the vicinity of the stress concentration, such as micro cracks. Moreover, the glassy phases concentrated in the BN layer and which might happen to plastic flow on the interface layer. The two mechanisms may, meanwhile, effect the material creep. Tertiary, or accelerated, creep is usually attributed to 'distributed' damage caused by nucleation, growth, and coalescence of cavities or microcracks, which gradually deteriorates the load-bearing capacity of the specimen. The lack of tertiary creep may suggest that fracture was dominated by localized damage due to the growth of preexisting defects, e.g. macrocracks or voids, even though other damaging mechanisms may operate concurrently. In other words, the growth of a defect to its critical size may usually happen before other damaging mechanisms start to have a significant effect on creep.[10] However, there was a difference between monolithic ceramic and fibrous monolithic ceramic. We know that fibrous monoliths are not governed by weak link statistics like monolith materials. For example, a few cells of a fibrous monolith can fracture without catastrophic failure occurring if the remaining cells can support the applied stress, so the tertiary creep of the Si_3N_4/BN fibrous ceramic does not appear.

There are many creep laws and thus many creep equations, none of which can describe the whole creep process. Usually, the creep strain rate ($\dot{\varepsilon}$) can be described by the power law:

$$\dot{\varepsilon} = A\sigma^n \exp\left(-\frac{Q}{RT}\right)$$

Where A is a constant, σ the stress, n the stress exponent for creep, Q the activation energy for creep, R the gas constant, and T the absolute temperature. The stress

Table 1
The rupture times of the composites at different temperatures under a variety of stresses

Temperature (°C)	Creep stresses (MPa)	Rupture times (h)
1000	250	>300
	350	>300
	400	>300
	500	50
	600	2
1100	250	>300
	350	>300
	400	>300
	500	16
	600	1.2
1200	250	>300
	350	210
	400	40
	500	4
	600	0.7

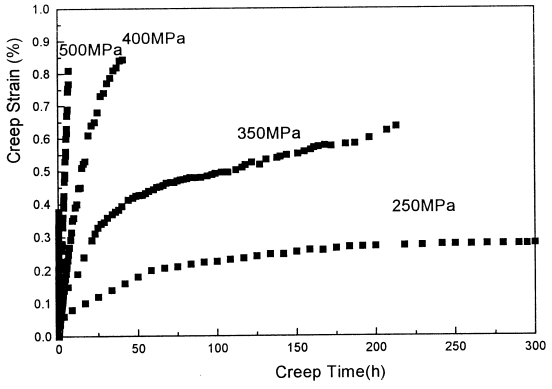

Fig. 1. The creep curves at 1200°C under different stresses.

exponent for the material is 1.69. It is usually considered that a number of deformation mechanisms, depending on the presence of grain boundaries, account for the creep behavior.[11] These include diffusion creep processes, grain boundary sliding controlled by the viscosity of the impurity phases at crystal boundaries, dissolution and redeposition of material and transfer of the viscous phases from boundaries under compression to those under tension. But the structure of Si_3N_4 fibrous monoliths was unique and obviously different from Si_3N_4 monoliths. Fibrous monoliths consisted of "soft" and "hard" phases. In Si_3N_4/BN fibrous monolithic ceramic, the "soft" phases were BN and the "hard" phases were Si_3N_4. The glassy phase was present in the boron nitride and the less glassy phase was present in the silicon nitride grains within the cells of fibrous monoliths as compared to silicon nitride grains in a monolithic specimen.[12,13] Therefore, the Si_3N_4/BN fibrous monoliths possess a low stress exponent and high creep resistance.

3.2. Microstructure observations and analysis

There are differences between the Si_3N_4/BN fibrous monolithic ceramic and monolithic Si_3N_4 ceramic in structure. The microstructure of Si_3N_4/BN fibrous monolithic ceramic is shown in Fig. 2(a) and (b). The polycrystalline Si_3N_4 cells and BN cell boundaries are viewed in the hot-pressing direction and normal to the hot-pressing direction.

In Si_3N_4/BN fibrous monolith, a major crack propagated through the specimen under tensile stress. Sometimes the major crack progressed through fibrous cells to the next interface. Sometimes it extended along the interface between fibrous cells. A branch-like crack could be observed in Fig. 3. The crack path was tortuous instead of line shaped. The branch-like crack makes the surface irregular and the surface area is increased. Therefore, it consumes more energy, which benefits creep resistance.

The microstructure of the materials observed by scanning electron microscopy (SEM) was illustrated in Fig. 4. It is observed that in the less glassy phase in Si_3N_4 grains, the cavities and voids were less on the grain boundary in Si_3N_4/BN fibrous monoliths, which could ascribe to the BN layers. The BN layers have capacity to absorb the glass and improve the creep resistance of the materials, but, as is well known, BN is unstable above 900°C, so the conclusion could be made that BN will lose that capacity. In order to examine the change in BN, we analyzed the XRD results obtained from the specimens after creep tests at high temperature under 400 MPa. It was found that BN stayed intact until 1200°C, so the BN interface improved the resistance to oxidation in the fibrous monoliths. At 1200°C, BN began to oxidise and formed B_2O_3. This reacted with Al_2O_3 and resulted in $2Al_2O_3{\cdot}B_2O_3$.

$$4BN(s) + 3O_2 \rightarrow 2B_2O_3(l) + 2N_2(g)$$

$$2Al_2O_3 + B_2O_3 \rightarrow 2Al_2O_3{\cdot}B_2O_3$$

The $2Al_2O_3{\cdot}B_2O_3$ formed strengthened the combination between BN and Si_3N_4. So with the temperature increased, although the creep rate was increased rapidly, the strength at 1200°C did not rapidly decrease.

The fracture surface of composite samples is illustrated in Fig. 5. Whisker pullout and crack deflection along the interface during fracture were indicated and the traces after the whisker pulled-out were observed. The Si_3N_4/BN fibrous monolithic ceramic was made by an extrusion process and hot pressing, the whiskers became aligned such that the major axes were preferentially oriented perpendicular to the direction of pressing. Whisker orientation affects the strength and fracture toughness of this material; therefore, its effect on creep deformation was investigated.[14] In the case of whisker-oriented alignment, most of the whiskers were perpendicular to the crack plane, i.e. parallel to the direction of stress, so that whiskers can effectively

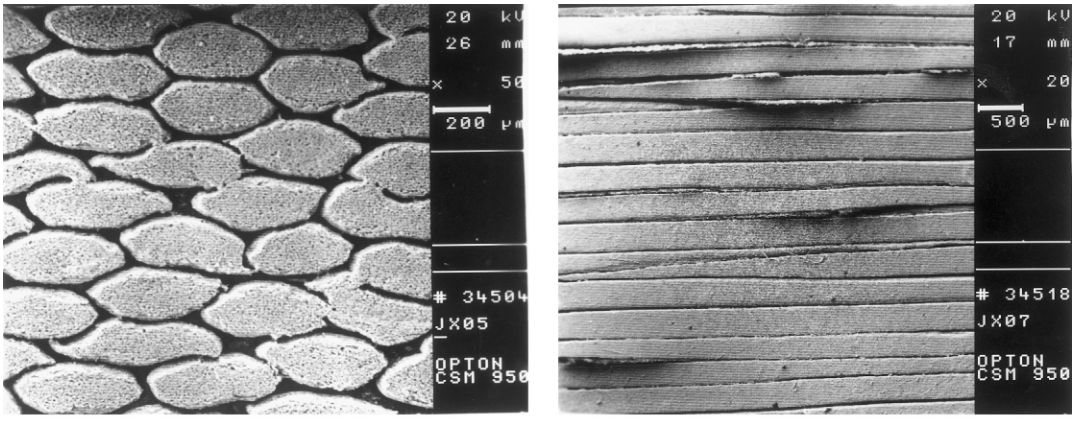

(a) (b)

Fig. 2. The microstructure of Si_3N_4/BN fibrous monolith. (a) Viewed in hot-pressing direction. (b) Viewed normal to the hot-pressing.

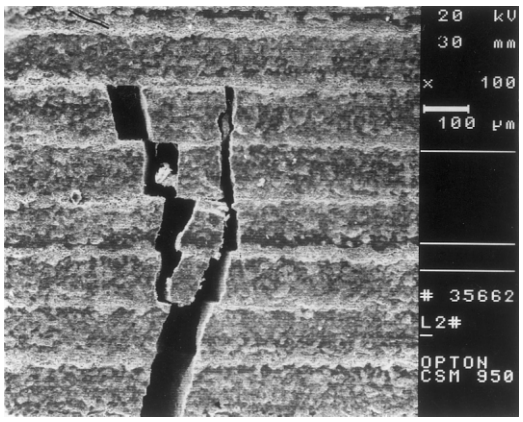

Fig. 3. A branch like crack in fibrous monolithic ceramics.

Fig. 4. The microstructure of Si_3N_4/BN fibrous monolith after creep under 350 MPa at 1200°C for 100 h.

Fig. 5. Fracture surfaces after creep test under 500 MPa at 1100°C for 16 h.

transfer stress and develop well. Consequently, debonding and whisker pulling-out will be observed in this case. The bridging ligaments carry part of the applied load by bridging the crack faces, leading to the reduction of effective driving stress of crack growth. The whisker improved the creep resistance greatly.

4. Conclusions

1. Si_3N_4/BN fibrous monolithic ceramics existed a substantial transient response in creep curve because the BN weak interlayer may facilitate the redistribution of stress.
2. BN interlayers had the capacity to absorb glass and purify the Si_3N_4 grain boundary. The creep deformation and fracture mechanisms were mainly controlled by the BN interlayer.
3. At 1200°C, the BN layer began to oxidise and form $2Al_2O_3{\cdot}B_2O_3$. The cavities and voids were increased more rapidly at 1200°C than at 1000 and 1100°C, which led to a decrease in creep resistance.
4. SiC whisker pulling-out greatly improved the creep resistance.

Acknowledgements

This work was supported by the National Natural Science Foundation of China (NSF).

References

1. Ziegler, G., Heinrich, J. and Wotting, G., Relationships between processing, microstructure and properties of dense and reaction-bonded silicon nitride. *J. Mater Sci.*, 1987, **22**, 3041–3080.
2. Mecholsky, J. J. Jr., Engineering needs of advanced ceramic-matrix composites. *Ceramic Bulletin*, 1989, **68**, 1083–1099.
3. Clegg, W. J., Kendlaa, K. and Alford, N. M., A simple way to make tough ceramics. *Nature*, 1990, **347**, 445–447.
4. Huang, Y., Hao, H. N., Chen, Y. L. and Zhou, B. L., Design and preparation of silicon nitride composite with high fracture toughness and nacre structure. *Acta Metall. Sinica*, 1996, **9**, 479–484.
5. Goto, Y. and Tsuge, A., Mechnical properties of unidirectionally oriented SiC-whisker-reinforced Si_3N_4 fabricated by extrusion and hot-pressing. *J. Am. Ceram. Soc.*, 1993, **76**, 1420–1424.
6. Matsui, T., Komora, O. and Miyake, M., The effects of surface coating and orienting of whiskers on mechanical properties of SiC(w)/Si_3N_4. *J. Ceram. Soc. Jpn.*, 1991, **99**, 1103–1109.
7. Guo, H., Huang, Y. and Wang, C., Preparation and properties of fibrous monolithic ceramics by in-situ synthesizing. *J. Mater Sci.*, 1999, **34**, 2455–2459.
8. Wu, X. and Holmes, J. W., Tensile creep and creep–strain recovery behavior of silicon carbide fiber/calcium aluminosilicate matrix ceramic composites. *J. Am. Ceram. Soc.*, 1993, **76**, 2659–2700.
9. Meyer, D. W., Cooper, R. F. and Plesha, M. E., High-temperature creep and the interfacial response of a ceramic-matrix composites. *J. Am. Ceram. Soc.*, 1996, **79**, 539–543.

10. Ding, J.-L., Liu, K. C. and Brinkman, C. R., Development of a high-temperature deformation and life prediction model for an advanced silicon nitride ceramic. *J. Am. Ceram. Soc.*, 1995, **78**, 3057–3066.
11. Birch, J. M. and Wilshire, B., The compression creep behaviour of silicon nitride ceramics. *J. Mater. Sci.*, 1978, **13**, 2627–2636.
12. Huang, Y., Guo, H. and Xie, Z. P., The fine micro-structure of interface layer for laminated Si_3N_4 ceramics. *J. Mater Sci. Lett.*, 1998, **17**, 569–571.
13. Trice, R. W. and Halloran, J. W., Elevated-temperature mechanical properties of silicon nitride/boron nitride fibrous monolithic ceramics. *J. Am. Ceram. Soc.*, 2000, **83**, 2735–2746.
14. Koester, D. A., Deformation and microstructural changes in SiC whisker-reinforced Si_3N_4 composites. *J. Mater Res.*, 1991, **6**(2).